

# Host Immune Response and Associated Clinical Features in a Primary Cytomegalovirus Eye Infection Model Using Anterior Chamber Inoculation

Chien-Chia Su,<sup>1-3</sup> Chia-Mao Gao,<sup>1</sup> Fu-Ti Peng,<sup>1</sup> Tzoo-Shuh Jou,<sup>2-4</sup> and I-Jong Wang<sup>1,3</sup>

<sup>1</sup>Department of Ophthalmology, National Taiwan University Hospital, Taipei, Taiwan

<sup>2</sup>Graduate Institute of Clinical Medicine, National Taiwan University, Taipei, Taiwan

<sup>3</sup>College of Medicine, National Taiwan University, Taipei, Taiwan

<sup>4</sup>Center of Precision Medicine, College of Medicine, National Taiwan University, Taipei, Taiwan

Correspondence: I-Jong Wang, No. 7, Chung-Shan S. Rd., Taipei, Taiwan; [ijong@ms8.hinet.net](mailto:ijong@ms8.hinet.net); Tzoo-Shuh Jou, No. 7, Chung-Shan S. Rd., Taipei, Taiwan; [jouts@ntu.edu.tw](mailto:jouts@ntu.edu.tw).

Received: January 18, 2022

Accepted: April 25, 2022

Published: May 17, 2022

Citation: Su CC, Gao CM, Peng FT, Jou TS, Wang IJ. Host immune response and associated clinical features in a primary cytomegalovirus eye infection model using anterior chamber inoculation. *Invest Ophthalmol Vis Sci.* 2022;63(5):18. <https://doi.org/10.1167/iovs.63.5.18>

**PURPOSE.** To investigate the pathogenesis of cytomegalovirus (CMV)-associated anterior segment infection in immunocompetent hosts and evaluate the effects of ganciclovir and glucocorticoid treatment in management of the disease.

**METHODS.** We used an inoculation model to reproduce CMV anterior segment infection in immunocompetent rats. Flow cytometry, cytokine analysis, histopathological sections, and quantitative polymerase chain reaction were performed to investigate the immune response after CMV infection. The effects of ganciclovir and glucocorticoid treatment were also assessed.

**RESULTS.** Anterior chamber inoculation of CMV in rats provoked characteristic pathological features of human CMV anterior segment infection. The innate and adaptive immunity sequentially developed in an anterior segment after inoculation, and the elevation of intraocular pressure (IOP) was highly associated with ocular infiltration and inflammation. Early ocular immune response reduced virus DNA in the anterior segment and alleviated viral lymphadenopathy. Early intervention with ganciclovir enhanced the release of cytokines associated with T response and facilitated recruitment of NKT and T cells in drainage lymph nodes. Glucocorticoid treatment, alone or combined with ganciclovir, decreased elevation of IOP but also impeded DNA clearance.

**CONCLUSIONS.** The inoculation model reproduced characteristic pathological features of human CMV anterior segment infection. The use of glucocorticoid in current practice may hinder viral clearance, and ganciclovir therapy can assist cytokine expression to combat the virus.

Keywords: cytomegalovirus, intraocular pressure, innate immunity, adaptive immunity

Cytomegalovirus (CMV)-associated infection in the anterior segment of the eyes in immunocompetent patients presents with the specific characteristics,<sup>1</sup> including anterior uveitis with anterior chamber inflammation and keratic precipitates (KPs), elevated intraocular pressure (IOP), and corneal endothelium cell damage, which are notably different from the manifestation of immunocompromised patients.<sup>2</sup> Clinical findings such as a typical owl's-eye appearance around the lesion of corneal endothelium on confocal microscopy<sup>3</sup> destroyed trabecular meshwork and sectoral iris atrophy<sup>4</sup> have implied a mechanism of direct viral invasion into ocular tissues.

Although the pathogenesis of CMV-associated anterior segment infection remains unknown, the normal physiological function of corneal endothelium and trabecular meshwork is surely disturbed after infection. Our previous study found that CMV-positive eyes with longer disease duration have poor control of IOP and may require glaucoma-filtering surgery even after eradication of CMV with long-term topical ganciclovir therapy.<sup>5</sup> In line with these clinical findings, a

recent study using CMV AD169 strain to infect human trabecular meshwork cell culture has demonstrated that cytopathic features such as disorganization and decreased cellularity of meshwork cells, enhanced production of transforming growth factor- $\beta$ 1, a pathogenic cytokine to reduce extracellular matrix turnover, increased meshwork cell contraction, and increased outflow resistance.<sup>6</sup>

Human CMV establishes a lifelong latent infection after primary infection and may be periodically reactivated. Voigt et al. demonstrate broad ocular infection, chronic inflammation, and a latent viral reservoir after systemic murine CMV infection by intraperitoneal injection of CMV virus stock.<sup>7</sup> In previous studies using anterior chamber inoculation model, Bale et al.<sup>8</sup> has demonstrated murine CMV DNA exists in cells of the iris, ciliary body, and, rarely, the retina or choroid on days 4 and 7 of infection in immunocompetent mice. The tissue tropism revealed by this model reflects the clinical finding of CMV-associated anterior segment infection. Nonetheless, the relationship of IOP elevation and immune response in CMV-associated anterior segment

infection remains unclear. In the current study, we investigated the pathogenesis of CMV-associated anterior segment infection. We compared the clinical feature, especially IOP elevation, of CMV infection using anterior inoculation or systemic infection. We used the anterior chamber inoculation model and treatment with local glucocorticoid (GC) or ganciclovir to clarify the role of the immune response in IOP elevation and viral clearance.

## MATERIALS AND METHODS

### Reagents

Phosphate-buffered saline solution (PBS), trypsin, DAPI, and Alexa Fluor 546 phalloidin were purchased from Invitrogen Corp. (Carlsbad, CA, USA). Alexa Fluor 647-conjugated anti-CD3 (clone 1F4), PE-conjugated anti-CD11b/c (clone OX-42), PerCP-conjugated anti-CD8 (clone OX-8), APC/Cy7 conjugated anti-rat CD4 (clone W3/25), PE/Cy7-conjugated anti-rat CD45 (clone OX-1), and PE-conjugated anti-CD161 (clone 3.2.3) were purchased from BioLegend (San Diego, CA, USA).

Antibodies used in histologic section included: anti-cytomegalovirus antigen (BSB 5454; Bio SB, Santa Barbara, CA, USA); anti-CD3 (DB 082; DB Biotech, Kosicky, Slovakia); anti-CD4 (MCA55R), and anti-CD8 $\alpha$  (MCA48R) from Bio-Rad (Hercules, CA, USA); and anti-CD161 (ab197979; Abcam, Cambridge, UK). To detect of cytomegalovirus DNA in situ hybridization, digoxigenin-labeled CMV probe (T-1113-400) was obtained from ZytoVision GmbH (Bremerhaven, Germany).

### Virus Amplification and Plaque Assay

The Rat2 cell line (CRL-1764) and Rat CMV Priscott strain (VR 991) were purchased from the American Type Culture Collection (Rockville, MD, USA) and cultivated in Dulbecco's modified Eagle's medium with 5% fetal bovine serum at 37°C in a humidified chamber containing 5% CO<sub>2</sub>. Rat2 cells were cultivated in 24-well plate until more than 90% confluent and then exposed to serum starvation for 24 hours before CMV of specific titer was inoculated. After two hours, virus medium with Dulbecco's phosphate-buffered saline solution buffer containing no calcium and magnesium cation was replaced. Then, Dulbecco's modified Eagle's medium with 1% fetal bovine serum and 1% methylcellulose was added and cells were kept cultivated until the plaques could be enumerated. When viral cytopathic effects were visible to be approximately 20~80 per well, cells were fixed with ice-cold methanol for 30 minutes. After adding methylene blue for 30 minutes, the virus titer was quantitated by estimating the number of plaque-forming cells in the infected culture. Plaque-forming unit (PFU) per millimeter was determined before the virus-containing supernatant was stored with 35% sorbitol in -80°C for further usage.

### Animals

Six-week-old male Sprague-Dawley rats were obtained from the Animal Resources Center (Lasco, Taiwan) and were kept under pathogen-free conditions. Food and water were supplied as desired. All procedures followed local animal welfare regulations according to the Association for Research in Vision and Ophthalmology statement for the use of research animals.

### CMV Infection

Animals were anesthetized with inhalation of oxygen and nitrous oxide (4:1) and intramuscular injection of xylazine (Ropum 2%, 5.6 mg/kg; Bayer Suisse, Lyssach, Switzerland) and tiletamine plus zolazepam (Zoletil 50, 18 mg/kg; Virbac of Brazil, São Paulo, Brazil). Systemic infection was provoked by intraperitoneal injection of 10<sup>5</sup> PFU virus stock of CMV (n = 10). Anterior segment CMV infection was elicited by anterior chamber inoculation model. In brief, intracameral injection (IC) of 0.01 mL virus stock of CMV (10<sup>5</sup> and 10<sup>5</sup> PFU) (n = 10, each) was done after instillation of 0.5% Alcaine Ophthalmic Solution (Alcon, Fort Worth, TX, USA) into the right eye of each rat to minimize blink reflex.

The IOP was measured by rebound tonometer (Icare TonoLab, Vantaa, Finland) every day post-infection for 12 days. To investigate the effect of different treatments on IOP elevation, rats were divided into three groups (n = 10 in each group). The primary CMV infection was induced by IC injection of 0.01 mL CMV virus (10<sup>5</sup> PFU), 0.02 mL of 2 mg/mL ganciclovir was injected intravitreally four hours after infection in group 1, whereas intravitreal injection of 0.02 mL of 40 mg/mL methylprednisolone sodium succinate (MPSS) was performed four hours after infection with replenishment of 0.02 mL of 40 mg/mL MPSS every other day in group 2. Concomitant 2 mg/mL ganciclovir and 40 mg/mL MPSS was given four hours after infection with replenishment of 0.02 mL of 40 mg/mL MPSS every other day in group 3. The measurement of IOP was performed every day after infection for six days.

### Aqueous Humor Sampling for Flow Cytometry

After rats were sacrificed, the eyes were cleaned, and aqueous humor was collected with 31G syringes. A total of 80  $\mu$ L aqueous humor from four rat eyes was placed in 1.5 mL microcentrifuge tubes on ice. After centrifugation at 300g for 10 minutes at 4°C, the supernatant was discarded, and the cells were resuspended in 1 mL of cell staining buffer (cat. 420201; BioLegend). The total cell number was counted with a hemocytometer. A fixed proportion volume of staining buffer was added to make a diluted concentration of 10<sup>5</sup> cell/300  $\mu$ L in each sample. Each sample was well mixed and aliquot 300  $\mu$ L of the sample was prepared for flow cytometry, according to manufacturer's instructions, with the indicated antibodies. Data were processed using CellQuest software (BD Biosciences).

### Lymph Node Sample for Flow Cytometry

After euthanization of the rats, superficial and deep cervical lymph nodes were collected and homogenized. After filtration with cell strainer (Falcon), the homogenates were spun in a centrifuge at 200g for 10 minutes at 4°C. The supernatant was discarded and the cells were immersed in 1 mL of cell staining buffer (cat. 420201; BioLegend). The total cell number was counted by hemocytometer. A fixed proportion volume of staining buffer was added to make a diluted concentration of 10<sup>6</sup> cell/300  $\mu$ L in each sample. Each sample was well mixed and aliquot 300  $\mu$ L of the sample was prepared for flow cytometry, according to manufacturer's instructions, using the indicated antibodies. Data were processed using CellQuest software (BD Biosciences).

### Cytokine/Chemokine Magnetic Bead Panel

The whole blood was retrieved from inferior vena cava and was centrifuged at 130g for 10 minutes at room temperature to separate plasma for the following assay. The Milliplex Rat Cytokine/Chemokine Magnetic Bead Panel kit (EMD Millipore, Darmstadt, Germany) was used to detect the indicated cytokines. The whole corneal button along with uvea tissue was collected and kept frozen. The anterior segment tissue was ground in liquid nitrogen using a chilled mortar and pestle. Lysis buffer 1 mL (cat. 43-040, Milliplex) with Protease Inhibitor cocktail (cat. 04 693 132 001, Roche) was added to 50 to 100 mg ground tissue. Each sample was incubated on rocker at 4°C for 15 minutes and then spun in a centrifuge at 10,000g for 10 minutes at 4°C. An aliquot of each sample was quantified for total protein concentration with colorimetric assay (Protein Assay Kit, Bio-Rad). The concentrations of cytokines and chemokines were determined according to the instruction from manufacturer by a linear curve fit.

### Immunofluorescence

The whole eyeball was embedded in Tissue-Tek OCT medium (Sakura Finetek, Torrance, CA, USA). Ten-micrometer sections were fixed in 4% paraformaldehyde for 10 minutes, blocked with 5% BSA in PBS, and incubated with the following primary antibodies at 4°C overnight: mouse anti-rat CD4 (MCA55R; Bio-Rad), mouse anti-rat CD8 $\alpha$  (MCA48R; Bio-Rad), rabbit anti-CD161 (ab197979; Abcam). After washing twice with PBS for 15 minutes, samples were incubated with FITC-conjugated secondary antibody (cat. A-11001; Invitrogen) (1:100) at room temperature for one hour. Cell nuclei were counterstained with DAPI. Confocal images were taken using Leica TCS SP5 confocal microscope.

### Immunohistochemistry and Hematoxylin and Eosin Staining

The eyeball and dissected lymph nodes were perfused with PBS followed by 4% paraformaldehyde overnight to be processed for paraffin embedding. Five-micrometer sections were cut from the paraffin blocks, mounted on glass slides, and labeled with mouse anti-rat CD3 (DB-082; DB Biotech) and anti-cytomegalovirus antigen (BSB 5454; Bio SB). A Horseradish Peroxidase Labeling Kit (TAHC03D; BioTnA, Kaohsiung City, Taiwan) was used for detect diaminobenzidine staining. Paraffin sections were stained hematoxylin and eosin staining. Images were obtained with MoticEasyScan Pro (Motic Asia, Hong Kong) and processed with EasyScanner software.

### Vital Dye Staining

The corneal buttons of rats were retrieved with scissors and washed by sterile balanced salt solution (Alcon Laboratories, Geneva, Switzerland). The corneal endothelial layer was immersed with drops of 0.4% trypan blue for 60 seconds. The corneal button was rinsed with balanced salt solution twice, immersed with 0.5% alizarin red for 180 seconds, and rinsed with balanced salt solution twice again before being observed under a bright field microscope.

### Real-Time Quantitative Polymerase Chain Reaction

The first set of primers were the forward primer (5'-TTCGCTTCGGTGATGGAACA-3') and the reverse primer (5'-CGTGGCCTGTAACATCTGGT-3') targeting 312 bp of intron region in immediate-early (IE) gene with the reference sequence U62396.<sup>9</sup> The primers were designed using Primer3. The second set of primers were the forward primer (5'-ATGACATCAAGAAGGTGGTG-3') and the reverse primer (5'-CATACCAGGAAATGAGCTTG-3') targeting GAPDH gene according to the previous reference.<sup>10</sup>

CMV-infected eyes were dissected into the cornea, anterior uvea (iris and ciliary body), and retina parts that were separately processed for parallel RNA and DNA purification using NucleoSpin RNA/DNA Buffer Set (Macherey-Nagel, Düren, Germany). Real-time reverse transcription-polymerase chain reaction (RT-PCR) (TaqMan one-step RT-PCR master mix reagents kit; Applied Biosystems, Foster City, CA, USA) was performed and the RNA transcript of immediate-early gene was quantitated using Applied Biosystems 7300 Fast RT-PCR system (Applied Biosystems) with the following cycling condition: hot start at 95°C for two minutes, followed by 40 cycles of denaturation at 95°C for five seconds, and combined annealing and extension at 60°C for 30 seconds. The real-time PCR was performed to analyze the DNA of IE gene with similar PCR protocol. Data acquisition and analysis were using CFX Manager software. All DNA and RNA levels were normalized to GAPDH.

### Statistics

The data are expressed as mean  $\pm$  SEM. Differences between groups were compared by using the Mann-Whitney U test and Student's *t* test. Values of *P* < 0.05 were considered to indicate statistical significance.

## RESULTS

### Anterior Chamber Inoculation of CMV in Rats Provoked Characteristic Pathological Features

The IOP was monitored daily after anterior segment rat CMV infection in susceptible rats that revealed IOP fluctuated post-infection in a biphasic fashion with peaks noted on day 2 and day 9. Higher virus titer ( $10^5$  PFU) inoculation elicited a greater IOP elevation, compared to lower virus titer ( $10^5$  PFU). By contrast, systemic rat CMV infection with an intraperitoneal injection ( $10^5$  PFU) did not increase in IOP (Fig. 1A, upper panels) highlighting the effect of infectious route on developing the characteristic IOP elevation commonly observed in the CMV infected eyes of human subjects.<sup>5,11</sup> The examination of external rat eyes performed on day 6 disclosed characteristic localized corneal edema<sup>12</sup> only in rats with anterior chamber inoculation of CMV but not in rats with systemic CMV infection (Fig. 1A, lower panels). The rat corneal buttons harvested on day 12 revealed pathognomonic features of multinucleated endothelial cell<sup>13</sup> in the cornea of rats with anterior chamber inoculation (Figs. 1B, 1C). In line with the above pathological findings that implied the existence of CMV infection, both CMV antigens and genomes were documented in the trabecular meshwork and wall of Schlemm's canals of eyes from rats infected by CMV through anterior chamber inoculation (Figs. 1D, 1E). The inflammatory cells were predominantly

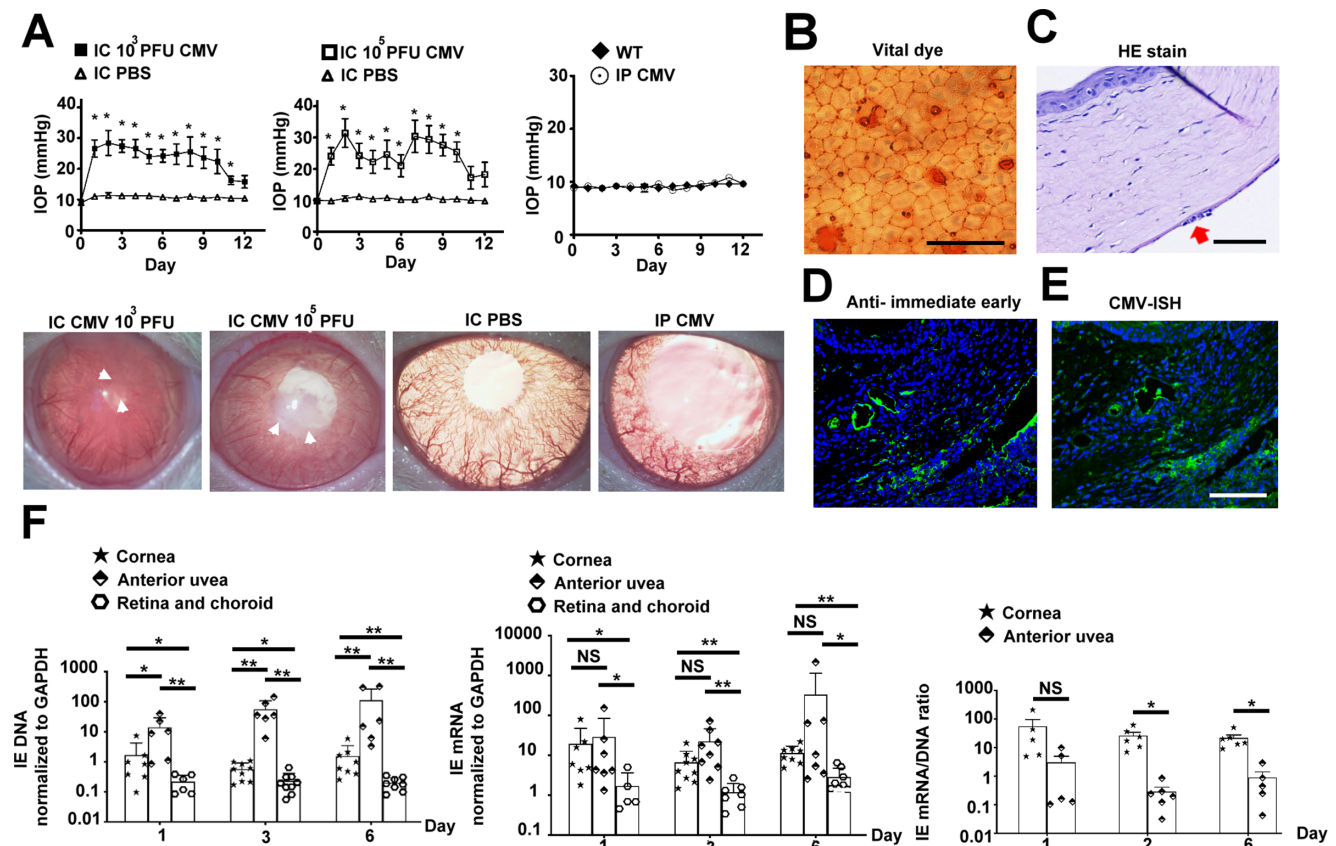


**FIGURE 1.** Pathological changes in the anterior segments of rat eyes after CMV infection. Primary CMV infection was induced by IC injection of 0.02 mL CMV virus ( $10^3$  and  $10^5$  PFU) or by intraperitoneal injection ( $10^5$  PFU) ( $n = 10$ , each). Control rats received intracameral injection of 0.02 mL PBS ( $n = 10$ ). (A) Rodent IOP was measured by TonoLab tonometer from day 1 to day 12 after infection. Representative external eye photographs from each group were taken six days after infection. The opacified region due to corneal edema was marked with *white arrowheads*. (B) The rat corneal buttons harvested on day 12 were processed for vital dye staining. (C–E) The anterior segments were processed for hematoxylin and eosin staining (multinucleated cells were indicated with an *arrow*), and for immunofluorescent staining using specific antibody detecting CMV antigen and CMV fluorescence in situ hybridization (ISH). (F) CMV immediate early gene DNA and RNA as well as the IE RNA/DNA ratio in the indicated eye compartments was detected and quantified by qPCR at day 1, day 3, or day 6 post-infection ( $n = 5\sim 8$ ). Scale bar: 100  $\mu\text{m}$  \* $P < 0.05$ ; \*\* $P < 0.01$ .

noted in the anterior segment, iris, and ciliary body without any sign of retinitis (Supplementary Fig. S1). Taken together, these data established our experimental scheme as a legitimate model that can reproduce the pathogenesis of CMV eye infection.

We next assessed the amount of CMV immediate-early gene DNA and RNA transcripts in separate eye compartments at days 1, 3, and 6 after infection. The highest CMV DNA was detected in the ciliary body and iris (anterior uvea), followed by the cornea, and least viral DNA was present in the retina and choroid (Fig. 1F). Quantitation of RNA transcripts, as well as the ratio of RNA/DNA, followed a similar distribution pattern.

### Innate and Adaptive Immune Cells Infiltrate Sequentially in Aqueous Humor After Anterior Segment CMV Infection

To delineate local immune response in the anterior chamber after CMV infection, we directly assessed the profiles of inflammatory cells in aqueous humor. There was a marked infiltration of inflammatory cells on days 2 and 6, as demonstrated by histological sections of iridocorneal

angle (Fig. 2A) and an increase in  $\text{CD45}^+$  cells by flow cytometry (Fig. 2D). Compared to control eyes, immunofluorescence staining of the iridocorneal angle displayed a pronounced surge of natural killer cells on day 2 after infection, which quickly decreased, whereas  $\text{CD4}^+$  T and  $\text{CD8}^+$  T cells increased later during CMV infection (Fig. 2C). Further detailed analysis showed that the antigen-presenting  $\text{CD11bc}^+$  cells and natural killer cells comprised the majority of cells in aqueous humor at the earlier phase of infection; however, these innate immune cells decreased significantly by day 6 after infection (Figs. 2B, 2F). In contrast to the profiling of innate immunity, the adaptive immune cells, including  $\text{CD4}^+$  T cells,  $\text{CD8}^+$  T cells, and NKT cells, gradually increased in their absolute numbers and percentage during the course of observation (Figs. 2B, 2F). The bivariate plot of flow cytometry clearly demonstrated a shift of natural killer cells to  $\text{CD3}^+$  T cells during CMV infection (Fig. 2E).

### Local But not Systemic Cytokines Were Involved in the Host Immune Response to CMV Infection

To identify the source of the humoral factors involved in triggering above mentioned cellular infiltration into the anterior segment tissue after CMV infection, we examined multiple

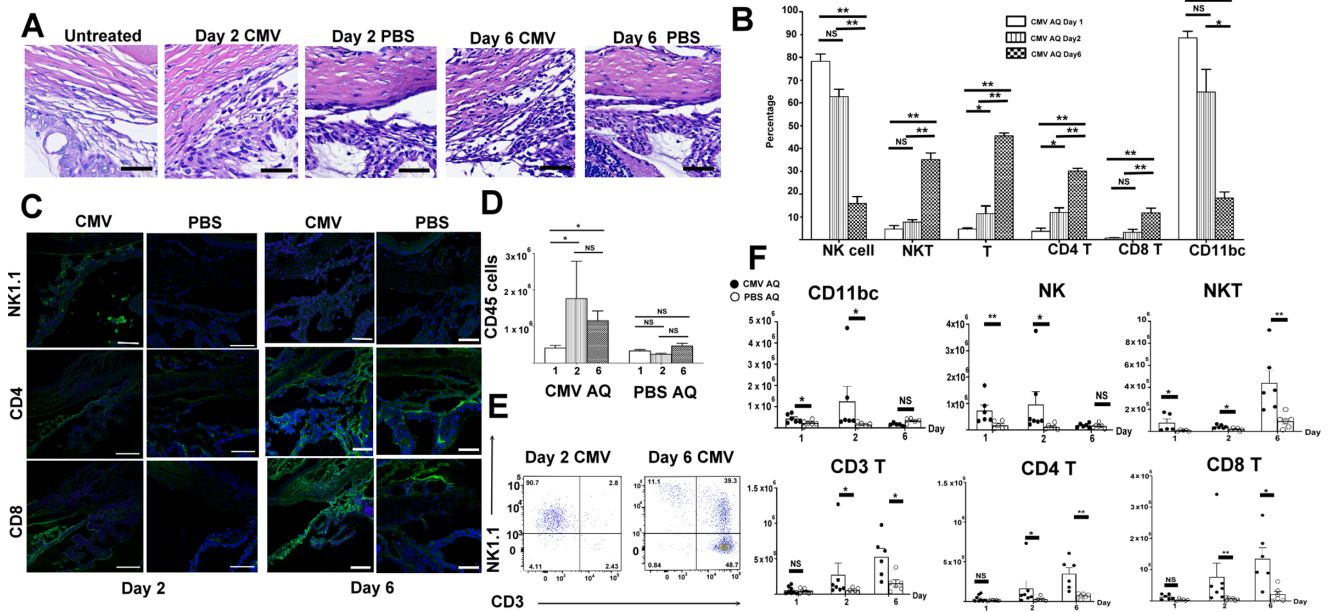


**FIGURE 2.** Innate and adaptive immune cells infiltrated sequentially in aqueous humor after anterior segment Rat CMV infection. Primary CMV infection was induced by intracameral injection of 0.02 mL CMV virus ( $10^5$  PFU). Control rats received intracameral injection of 0.02 mL PBS ( $n = 5\sim 8$ , each). (A) Representative histological sections of iridocorneal angle were taken on day 2 or day 6 in both groups and stained with hematoxylin and eosin. Scale bar: 50  $\mu$ m. (B) Single cell preparations from aqueous humor (AQ) at day1, day 2 and day 6 post-infection were prepared and stained for indicated cell markers. (C) The rats were sacrificed and processed for immunofluorescence staining using indicated antibodies on day 2 and day 6. Scale bar: 100  $\mu$ m. (D) Percentage of different cell types was calculated and compared between days. (E) Representative bivariate FACS plot of CD3<sup>+</sup>NK<sup>+</sup> expression by CD45<sup>+</sup> cells. (F) Absolute cell number of different cells was calculated and compared between groups and days. \* $P < 0.05$ ; \*\* $P < 0.01$ .

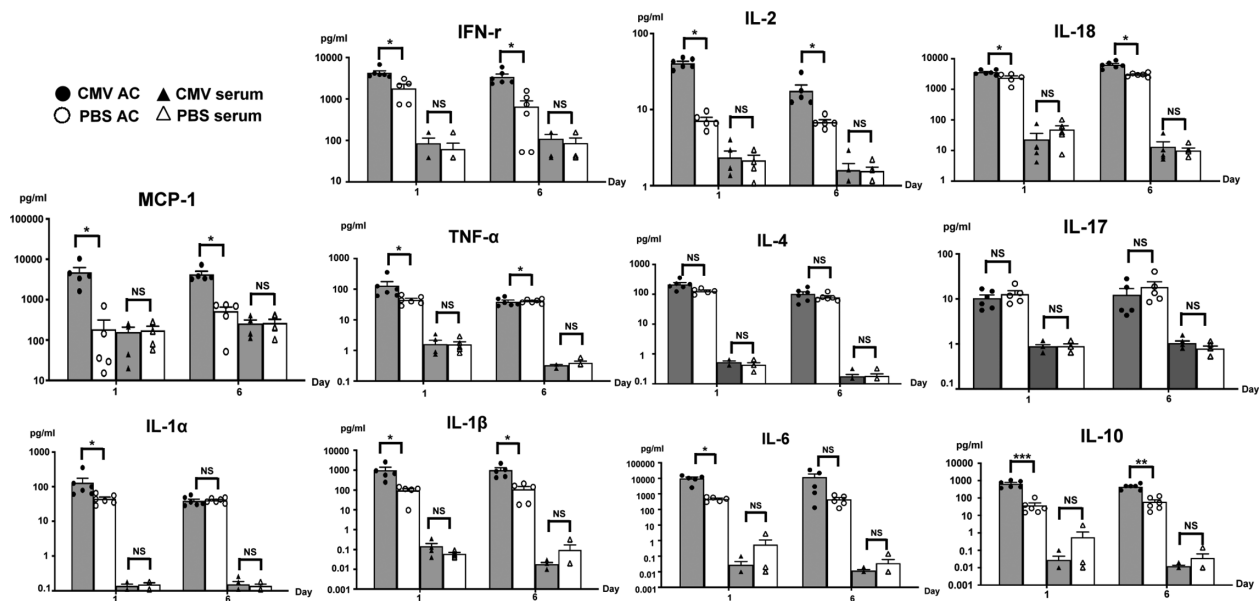


**FIGURE 3.** Local but not systemic cytokines were involved in eliciting the host immune response to CMV infection. Primary CMV infection was induced by intracameral injection of 0.02 mL CMV virus ( $10^5$  PFU). Control rats received intracameral injection of 0.02 mL PBS ( $n = 5\sim 8$ , each). The rats were sacrificed on day 1 and day 6 after infection. Tissue fluid retrieved from anterior segment and serum was possessed for cytokine magnetic bead panel. \* $P < 0.05$ ; \*\* $P < 0.01$ ; \*\*\* $P < 0.001$

chemokines and cytokines in both the anterior segment and plasma of the infected rats (Fig. 3). On day 1, MCP-1, IL-1 $\alpha$ , IL-1 $\beta$ , IL-2, IL-6, IL-10, IL-18, TNF- $\alpha$ , and IFN- $\gamma$  elevated

significantly in the tissue of anterior segment with CMV infection. On day 6, MCP-1, IL-1 $\beta$ , IL-2, IL-10, IL-18, TNF- $\alpha$ , and IFN- $\gamma$  remained significantly higher.

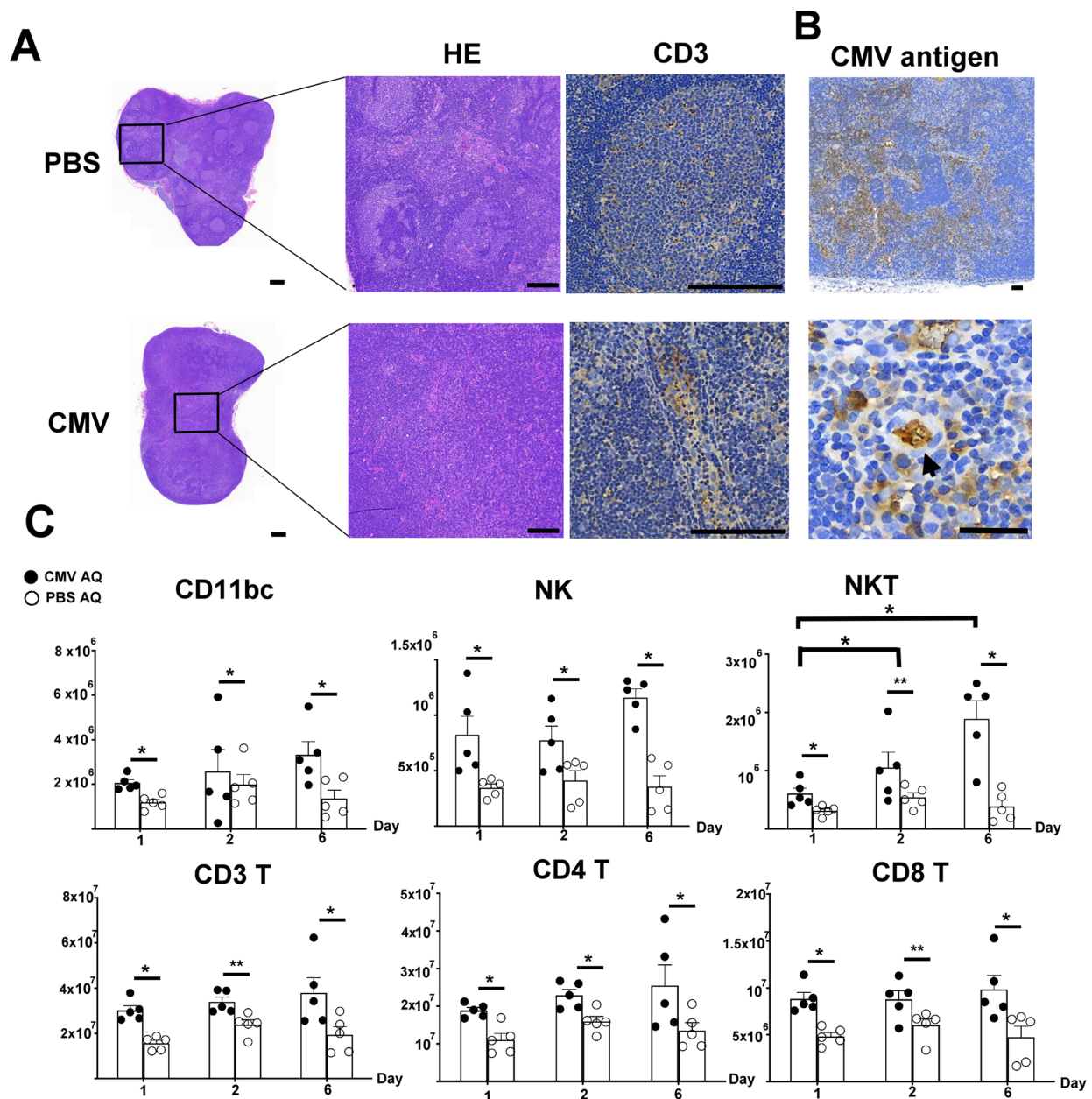


**FIGURE 4.** Viral lymphadenopathy developed in cervical lymph node after intracameral CMV infection. Primary CMV infection was induced by intracameral injection of 0.02 mL CMV virus ( $10^5$  PFU). Control rats received intracameral injection of 0.02 mL PBS ( $n = 5\sim 8$ , each). (A) Representative histological sections of lymph nodes were taken on day 6 in both groups, and stained with hematoxylin and eosin or processed for immunohistochemistry staining using CD3 antibody and specific antibodies detecting cytomegalovirus. Scale bar: 200  $\mu$ m. (B) The CMV antigen could be observed in the afferent lymphatic vessel (*upper panel*) and an owl's eye cell was indicated with an arrowhead (*lower panel*). (C) Single cell preparations from lymph nodes at day 1, day 2, and day 6 after infection were prepared and stained for the indicated cell markers for flow cytometry. Absolute cell number of different cells was calculated and compared between groups and days. \* $P < 0.05$ ; \*\* $P < 0.01$ .

### Viral Lymphadenopathy Developed in the Cervical Lymph Node After CMV Infection

To study the extraocular involvement of CMV eye infection, we collected the drainage lymph nodes and processed them for histological examination. In the noninfected control group, follicular hyperplasia without T cell expansion was found in the cervical lymph node, and the follicle margin was clear (Fig. 4A, upper panel). In stark contrast, a moth-eaten appearance with follicular depletion and parafollicular T cell

hyperplasia was observed in the lymph node section from the CMV group. The lymph vasculitis was also found (Fig. 4A, lower panel). These pathological findings were compatible with viral lymphadenopathy. Indeed, CMV immunoreactivity could be detected in the afferent lymphatic vessel (Fig. 4B, upper panel) with a characteristic owl's-eye feature (Fig. 4B, lower panel).

Given such an inflammatory pattern, we performed phenotypic screening of the resident cells in the drainage lymph nodes (Fig. 4C). The  $CD11bc^+$ , NK,  $CD4^+$  T,  $CD8^+$

T, and NKT cells in the CMV group all outnumbered those in the control group at every time point we surveyed after infection. Moreover, an increasing trend of NKT cell infiltration in the drainage lymph nodes was found from day 1 to day 6.

### GC Alleviated the Elevation of Intraocular Pressure but Also Impeded Viral DNA Clearance

We further investigated the effects of two mainstream treatments of CMV eye infection (GC and ganciclovir) on the disease course of our experimental rats. The IOP was reduced effectively by either GC, ganciclovir, or in combination (Fig. 5A, upper panel). The treatment with ganciclovir alone or in combination with GC abated localized edema completely on day 6 after infection. However, small opacified regions caused by corneal edema could still be observed in rat eyes treated with GC alone (Fig. 5A, lower panel). The amount of CMV DNA in the tissue decreased significantly from day 1 to day 6 after infection without any specific treatment signifying the capability of host immunity to combat the first wave of viral invasion in rat eyes (Fig. 5B). In contrast to ganciclovir, which did not affect the viral DNA clearance, GC usage, either alone or in combination with ganciclovir, significantly delayed viral DNA clearance. Treatment with GC, either alone or combining ganciclovir, significantly increased the CMV RNA expression in the tissue (Fig. 5B). Intriguingly, ganciclovir treatment reduced the viral IE RNA transcript in the tissue on day 6 after infection.

### Ganciclovir Alleviates Ocular Infiltrates and Enhanced Late Cytokine Release to Upregulate T Immune Response in the Drainage Lymph Nodes

Although both ganciclovir and GC could efficiently control the elevation of IOP following anterior segment CMV infection (Fig. 5A), the effect of GC was quite transient that it required continuous GC injection every other day to keep the IOP under check (i.e., IOP would rebound on the second day after one single dose of GC injection) (Supplementary Fig. S2). Unlike GC, one single dose of ganciclovir lowered down IOP throughout the experimental period. Ganciclovir treatment significantly decreased the infiltration of NK and CD11bc<sup>+</sup> cells, which were among the earliest inflammatory cells recruited to the CMV-infected eyes (Fig. 2), in the aqueous humor post-infection (Fig. 6A). In line with these findings, significant reduction in MCP-1 and IL-18, which have been demonstrated to facilitate recruitment of CD11 macrophage and priming of NK cells respectively,<sup>14,15</sup> was found in the anterior segment tissue of eyes treated with ganciclovir on post-infection day 1 (Fig. 7). The proinflammatory cytokines, such as IL-1 $\beta$  and IL-6, were also reduced with ganciclovir treatment on postinfection day 1 (Fig. 7).

Ganciclovir also reduced the CD11bc<sup>+</sup> cells in the drainage lymph nodes on post-infection day 1 (Fig. 6B). Although ganciclovir treatment alleviated the virus-provoked T cell population in the anterior chamber, several cytokines related to NKT and T cell responses (IL-1 $\alpha$ , IL-2, IL-18, TNF- $\alpha$ ) were significantly increased compared to other cytokines on post-infection day 6 (Fig. 7). Despite the effect of ganciclovir in the eye was to decrease the infiltration of immune cells, ganciclovir seemed to elicit greater immune responses with a significant increase in

NK cells and NKT cells and a trend of increasing T cells in the cervical lymph nodes on post-infection day 6 (Fig. 6B). Both ocular and extraocular infection had been identified in CMV inoculation model. Furthermore, intravitreal injection of ganciclovir reduced not only the viral load in the eye and thus eased inflammatory cells in the aqueous humor, but it also facilitated better immune defense against extraocular infection.

### Local GC Treatment Temporally Inhibited Ocular Infiltrates but Hampered Ganciclovir-Upregulated Cytokine Response and Subsequent NKT and T Lymphocytes Recruitment Into Regional Lymph Nodes

Local GC treatment inhibited both innate and adaptive immune cells infiltration into the aqueous humor after CMV infection (Fig. 6A). Treatment with GC alone or combined with ganciclovir significantly reduced expression of IL-18 and other pro-inflammatory cytokines, such as IL-1 $\beta$  and IL-6, at the early phase while suppressed expression of IFN- $\gamma$  at the late phase (Fig. 7). Notably, concomitant GC and ganciclovir treatment prevented the ganciclovir-dependent up-regulated cytokine responses (IL-1 $\alpha$ , IL-2, IL-18, TNF- $\alpha$ ) (Fig. 7), NKT cells recruitment as well as an increasing trend of T cell infiltration in the drainage lymph nodes on day 6 post-infection (Fig. 6B, right panels). These effects can potentially lead to an unfavorable delayed clearance of virus.

## DISCUSSION

This study used anterior chamber inoculation to investigate the clinical manifestation and immune response after primary CMV eye infection. The elevation of IOP after infection and characteristic pathologic findings support the appropriateness of current model in simulating clinical CMV infection of the anterior segment among immunocompetent subjects. Our histopathological and molecular biological findings documented CMV DNA mainly in iris, ciliary body, and cornea, but rarely in retina and choroid. This presentation of tissue tropism is similar to clinical findings of immunocompetent patients with CMV eye infection, who manifested the involvement at anterior segment as iritis, trabeculitis, and endotheliitis. The self-limited nature of CMV ocular infection depends on the innate and adaptive immunity built in the anterior chamber after infection. The current findings are in line with previous model inoculated with murine cytomegalovirus (MCMV),<sup>8</sup> which found MCMV DNA in cells of the iris, ciliary body, and rarely, the retina or choroid on days 4 and 7 of infection in immunocompetent mice. In contrast, abundant MCMV DNA was found in retinal layers in cyclophosphamide-treated mice on day 14 of infection.

The corneotrabeular endothelium, as well as uveal tissue, has been proposed as vulnerable tissues in this CMV-related anterior segment infection. In the current study, the multinucleated cells in corneal endothelium, as demonstrated in vital dye staining and HE section, also support the corneal endothelium is susceptible to CMV. The detection of CMV DNA in the corneal tissue confirmed the pathological findings and reflected the clinical presentation of owl's eye morphology and coin-shaped lesions in corneal endothelium from previous clinical reports.<sup>3,16</sup> In addition

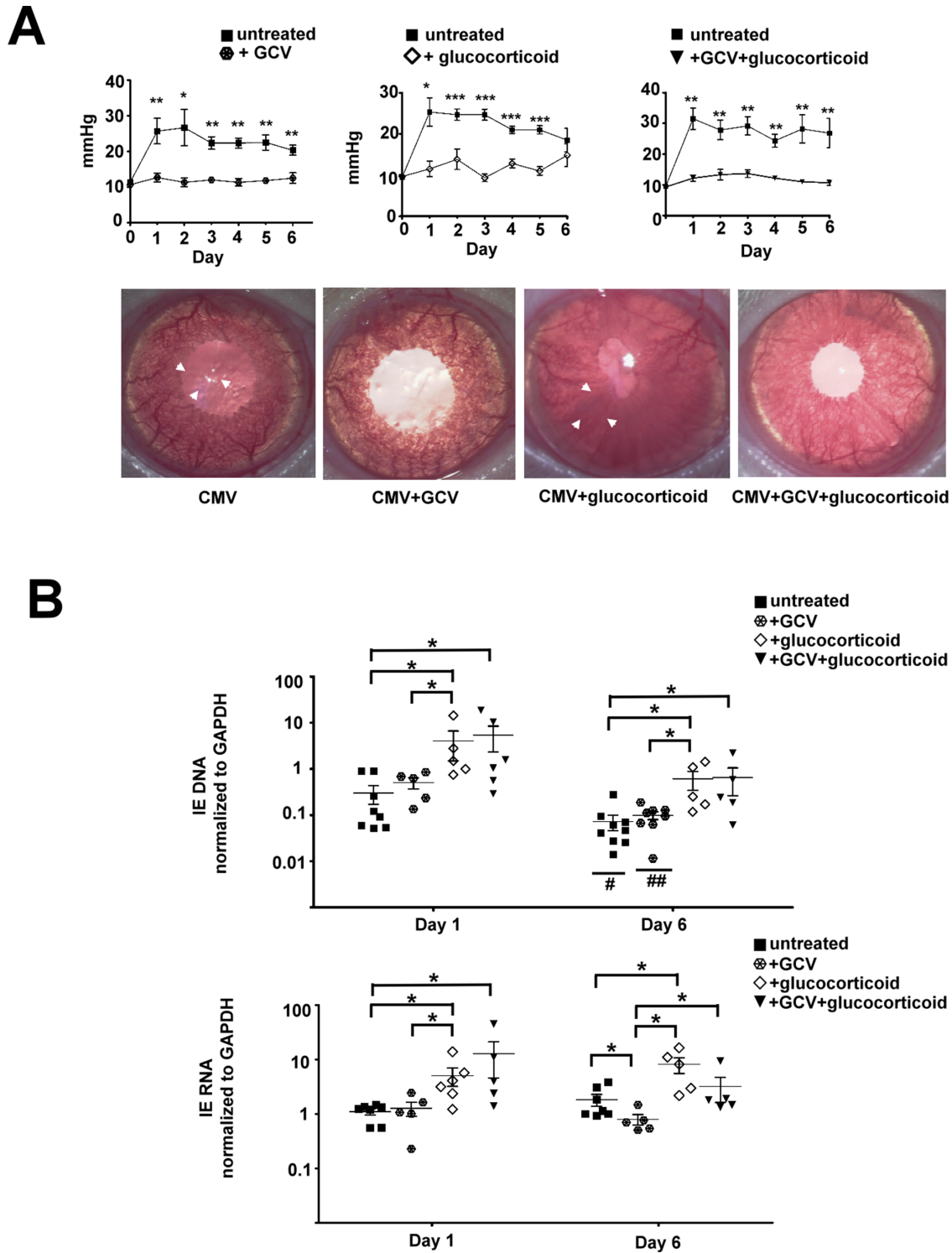


**FIGURE 5.** Glucocorticoid decreased elevation of intraocular pressure but also impeded DNA clearance. Primary CMV infection was induced by intracameral injection of 0.02 mL CMV virus ( $10^5$  PFU). These rats were divided into four groups and received intravitreal injections of 0.02 mL ganciclovir (2 mg/mL), or methylprednisolone sodium succinate (40 mg/mL), or combined ganciclovir (2 mg/mL) and methylprednisolone sodium succinate (40 mg/mL) ( $n = 10$ , each). (A) Rodent IOP was measured by TonoLab tonometer from day 1 to day 6 after infection. Representative external eye photographs from each group were taken six days after infection. The opacified region caused by corneal edema was marked with *white arrowheads*. (B) The presence of viral DNA and RNA in the anterior segment tissue was quantified by qPCR at day 1 and day 6 after infection ( $n = 5\sim 10$ ). The IE gene DNA and mRNA relative to GAPDH were quantified and compared between groups ( $*P < 0.05$ ;  $**P < 0.01$ ;  $***P < 0.001$ ) and between day 1 and day 6 ( $\#P < 0.05$ ;  $\#\#P < 0.01$ ).

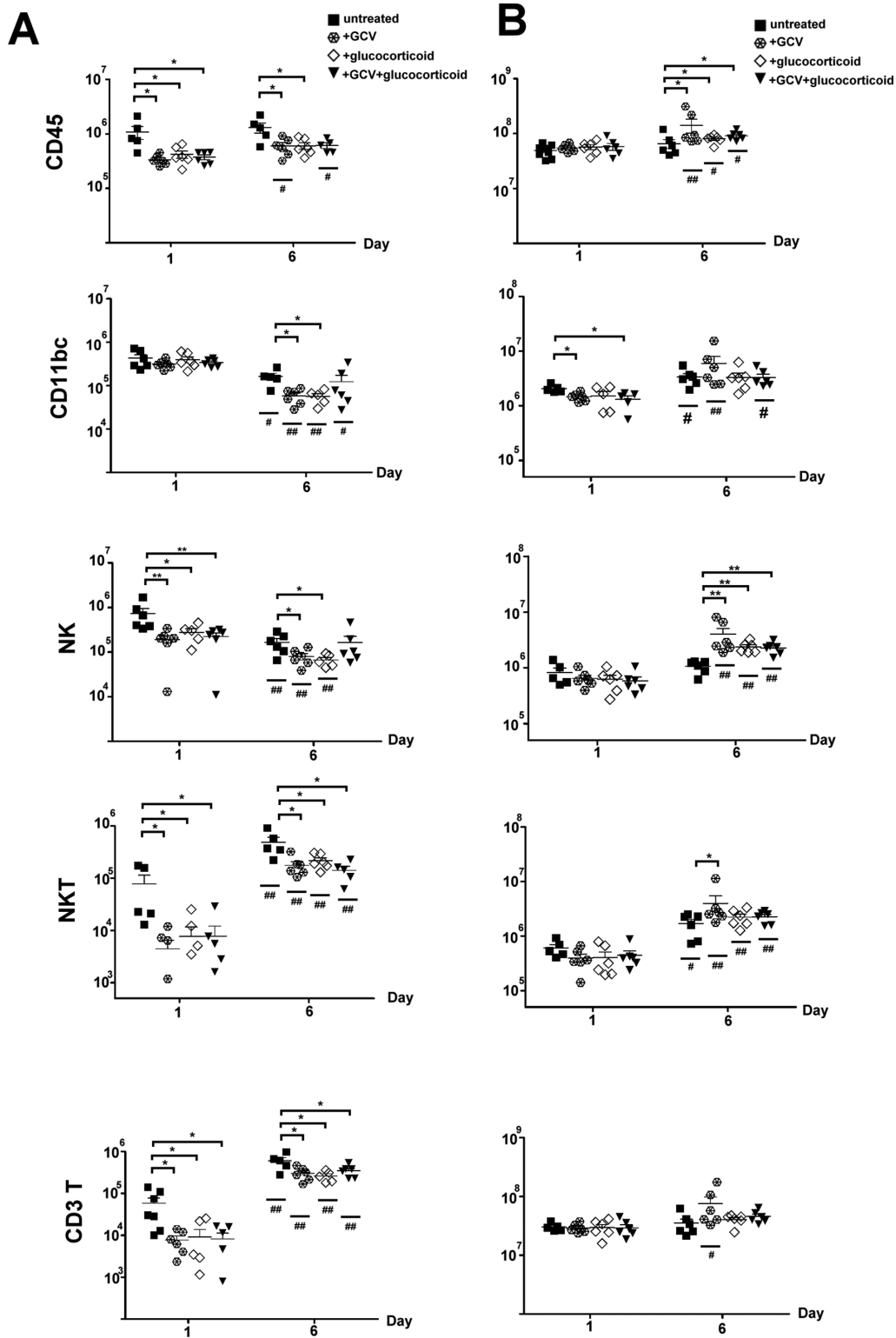


**FIGURE 6.** Early ocular immune response alleviated viral lymphadenopathy and ganciclovir treatment facilitated adaptive immune in drainage lymph node. Primary CMV infection was induced by intracameral injection of 0.02 mL CMV virus ( $10^5$  PFU). These rats were divided into four groups and received intravitreal injections of 0.02 mL ganciclovir (2 mg/mL) on day 1, or methylprednisolone sodium succinate (40 mg/mL) on day 2 and 4, or combined ganciclovir (2 mg/mL) and methylprednisolone sodium succinate (40 mg/mL) ( $n = 5\sim 7$ , each). Single cell preparations from aqueous humor (A) and drainage cervical lymph nodes (B) at day 1 and day 6 after infection were prepared and stained for the indicated cell markers before flow cytometry analysis. Absolute cell number of different cells was calculated and compared between groups (\* $P < 0.05$ ; \*\* $P < 0.01$ ) and days (# $P < 0.05$ ; ## $P < 0.01$ ).

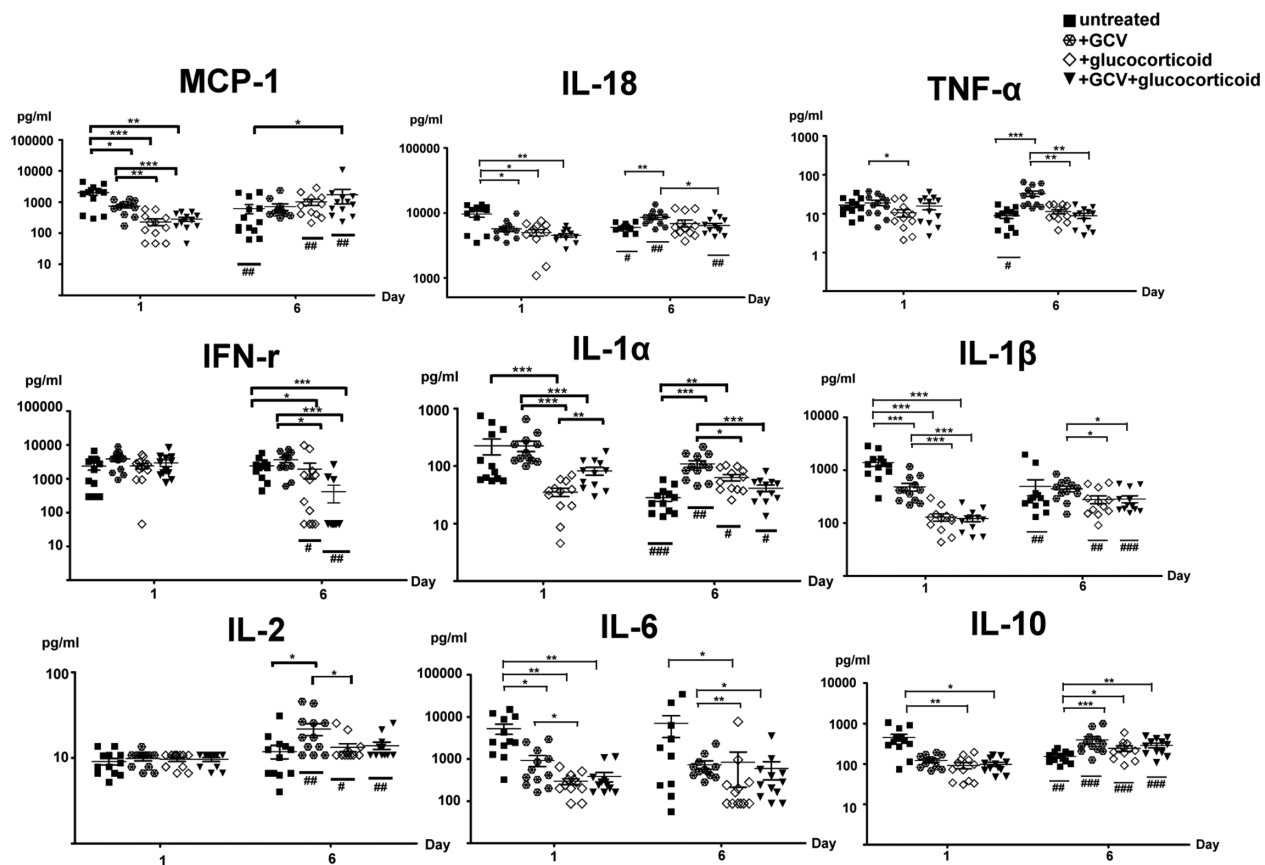


**FIGURE 7.** Ganciclovir treatment enhanced T cell immune responses through late cytokine release whereas concomitant glucocorticoid treatment hampered this process. Primary CMV infection was induced by intracameral injection of 0.02 mL CMV virus ( $10^5$  PFU). These rats were divided into four groups and received intravitreal injections of 0.02 mL ganciclovir (2 mg/mL) on day 1, or methylprednisolone sodium succinate (40 mg/mL) on days two and four, or combined ganciclovir (2 mg/mL) and methylprednisolone sodium succinate (40 mg/mL) ( $n = 10\sim 12$ , each). The rats were sacrificed on day 1 and day 6 after infection. Tissue fluid retrieved from anterior segment was possessed for cytokine magnetic bead panel. The cytokine level was compared between groups (\* $P < 0.05$ ; \*\* $P < 0.01$ ; \*\*\* $P < 0.001$ ) and days ( $^{\#}P < 0.05$ ;  $^{\#\#}P < 0.01$ ;  $^{\#\#\#}P < 0.001$ ).

to ocular tissue, a typical owl's-eye feature was detected in the vascular endothelium of drainage lymph nodes, implying a direct infection of drainage lymph nodes after primary anterior chamber inoculation. The antigens in the anterior chamber have been postulated to gain access to the lymphatic system via uveoscleral pathway through the loose subconjunctival connective tissue and reach the ipsilateral drainage lymph nodes of head and neck after intracameral injection.<sup>17,18</sup>

In the current study, the biphasic display of IOP could be rooted in the innate and adaptive immune responses built in the anterior chamber. The first peak of IOP correlated to the first wave of immune effector cells, mainly innate immune cells, including NK cells and antigen-presenting cells. After a transition from innate immunity to adaptive immunity, another IOP peaking around day 8 after infection may reflect a second wave of infiltration into the anterior segment by adaptive immune effectors, such as  $CD8^+$  T,  $CD4^+$  T, and NKT cells, which were disclosed in our analysis. The coinciding phenomenon of abridged ocular infiltrates and suppression of IOP in our experiments with antiviral or GC treatment further demonstrated the relationship between IOP and inflammatory cells. These findings elucidate the mechanism of IOP elevation in the acute CMV trabeculitis and show a similarity with the pathogenesis of herpes simplex

virus associated glaucoma, which also features a surge of IOP after infection that corresponds with a maximal anterior chamber immune reaction using a rabbit model.<sup>19</sup>

This study demonstrated  $CD11bc^+$  macrophages/dendritic cells infiltrated the anterior chamber at the early stage of CMV eye infection and it was accompanied by a regional rise of MCP-1 (CCL2), an important chemokine known to regulate migration and infiltration of monocytes.<sup>20</sup> These stimulated macrophages cells may not be originated from bone marrow because elevation of chemokines was only observed in local tissue, but not in the serum. This is distinguished from the case in systemic CMV infection, which recruits monocytes/macrophages from bone marrow.<sup>21,22</sup>

We also demonstrated that NK cells infiltrated to the anterior chamber with a surge of IFN- $\gamma$  and IL-18 on postinfection day 1 and day 2. NK cells are known to use the IFN- $\gamma$ -dependent mechanism as innate immunity against virus-infected cells in MCMV infection.<sup>23</sup> The findings of sustained elevation of IFN- $\gamma$  and IL-18 throughout postinfection day 6 also reflected that these two cytokines could be released from activated macrophages after CMV infection as demonstrated in previous MCMV infection.<sup>24</sup> Interestingly, the upregulation of these two cytokines in CMV-infected eyes with early ganciclovir therapy implies this

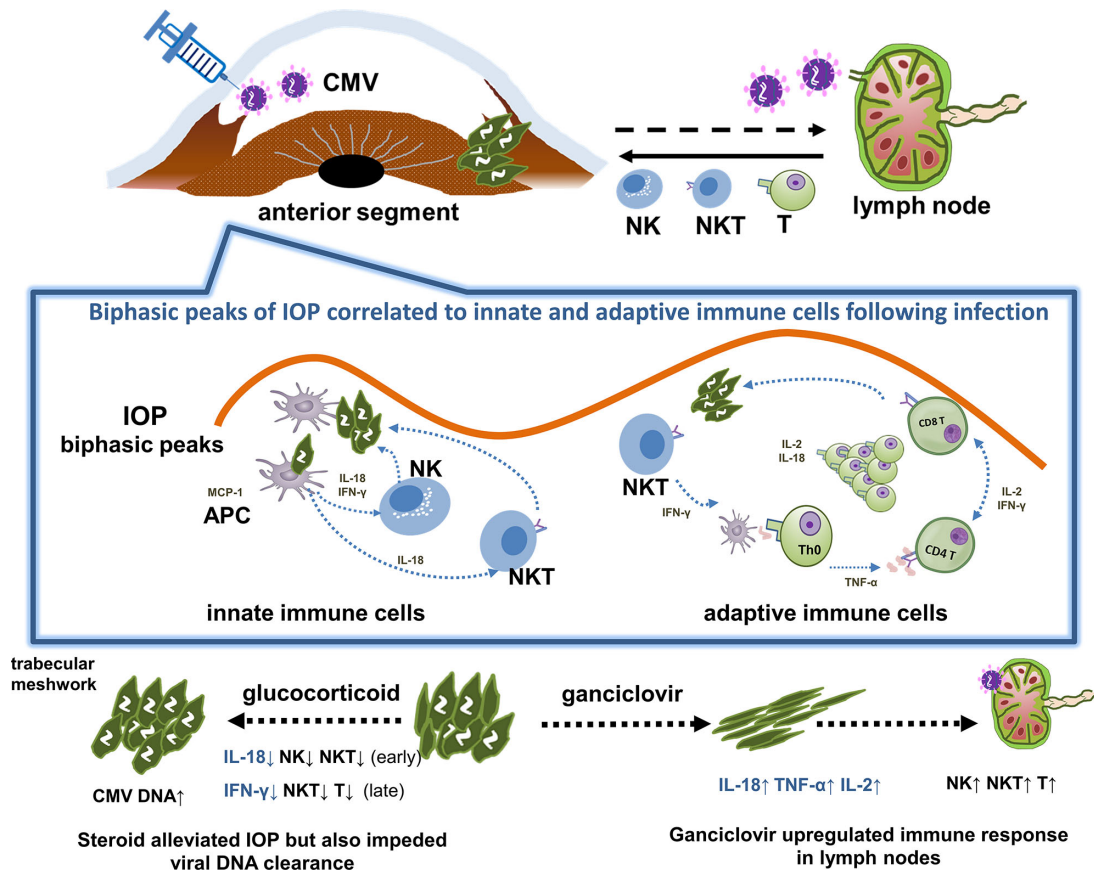


**FIGURE 8.** The host immune response in primary CMV anterior chamber inoculation. After inoculation, the elevation of intraocular pressure and gradual clearance of virus DNA in the anterior segment coincide with an inhibiting cascade of ocular immune cells resulting from the sequential development of innate and adaptive immunity against CMV infection. Glucocorticoid treatment hinders the viral clearance through preventing early recruitment of NK and NKT cells via downregulation of IL-18 and late recruitment of NKT and T cells via downregulation of IFN- $\gamma$ . Antiviral drug ganciclovir alone can upregulate several cytokines (TNF- $\alpha$ , IL-2, IL-18) to boost T cell response and facilitate expansion of NKT and T cells in drainage lymph nodes to limit CMV-associated damages.

could induce a beneficial effect on NK cells because IL-18 has been reported to prevent self-destruction of NK cells and enhance production of TNF- $\alpha$ , a pro-survival signal.<sup>25</sup> In addition, early ganciclovir treatment also enhanced expression of IL-2, an important cytokine released from adaptive CD4 T cells to augment NK cytotoxicity in CMV infection.<sup>26</sup> These findings suggest that the interplay between first-line antigen-presenting cells, NK cells, and T cells could be strengthened with early antiviral treatment in the incipient phase of acute CMV infection.

NKT cells, a critical link of innate and adaptive immune effectors and playing an instrumental role in facilitating CMV clearance, populated the anterior chamber soon after CMV inoculation. Our data demonstrated the increase of NKT cells was accompanied by elevation of IFN- $\gamma$ , but not IL-4 and IL-17, in the anterior chamber following CMV infection. These findings suggest that NKT cells have the capacity for rapid production of IFN- $\gamma$  and apparently behave like NK cells during the innate response against CMV infection.<sup>27</sup> The demonstration of a lack of IL-4 and IL-17 expression in the anterior chamber during expansion and activation of NKT cells in CMV eye infection also insinuates that activation of NKT cells can be cytokine driven and does not require engagement of T-cell receptor on antigen-presenting cells.<sup>28,29</sup>

Drainage lymph nodes are primary sites for early clonal expansion of antigen-specific T cells after intraocular antigen recognition. The appearance of parafollicular T-cell hyperplasia and lymph vasculitis in our studies concurs with previous reports and indicates that immunization in the anterior chamber, an immune-privileged site, induces T-cell clone expansion in the regional lymph nodes.<sup>30</sup> Although the anterior chamber is generally considered to be devoid of lymphatic drainage, several studies have shown that a connection between the eye and regional lymph nodes exists for both soluble<sup>17,31</sup> and nonsoluble antigens.<sup>32</sup> The presence of CMV antigen in the vascular endothelium of lymph nodes, as revealed in our study, suggests the CMV can be transmitted from anterior segment tissue to the afferent vascular endothelium.

In line with previous literature showing the detrimental effects of GC on most immune cells through activation of apoptosis pathways,<sup>33</sup> the present study found a significant reduction of immune cells, including NK cells, NKT cells, and T cells in eyes treated with GC (Fig. 8). Specifically, GC treatment significantly reduced the IL-18 level and the concomitant infiltration of NK and NKT cells in the anterior segment at the early phase. Moreover, GC treatment also significantly decreased IFN- $\gamma$  and the concurrent infiltration of NKT and T cells in the anterior chamber at the late phase.

Correspondingly, GC therapy alone or combined with antiviral treatment inhibited the viral clearance in the anterior segment.

In rats with ocular GC treatment, an increase of NK cells but not T cells was observed in the lymph nodes on postinfection day 6, implying more virus load in the afferent vascular endothelium because of less effective clearance in the ocular site. Nonetheless, the priming of T cells was influenced by GC treatment presumably because of impaired signaling from the anterior chamber. This finding concurs with the previous report that demonstrates the inhibitory effect of GC on lymphocytes as the treatment of mycoplasma uveitis using *Mycoplasma pulmonis* inoculation in the anterior chamber.<sup>34</sup> In our previous report,<sup>35</sup> we found that judicious use of topical steroid can be beneficial when used with protective topical ganciclovir in patients undergoing corneal transplantation with diagnosed CMV endotheliitis. The present study highlighted the GC treatment, alone or in combination with antiviral therapy, delayed clearance of viral DNA through downregulation of cytokines, and elicited more profound viral lymphadenopathy.

Ganciclovir (9-[(1,3-dihydroxy-2-propoxy) methyl] guanine) is a potent inhibitor of viruses of herpesviridae through selective inhibition of the viral DNA polymerase and subsequent blocking of viral DNA replication by the active metabolite ganciclovir-5'-triphosphate.<sup>36</sup> In the current study, the ganciclovir treatment hampered virus transcription and effectively reduced ocular infiltration of inflammatory cells. The demonstration that ganciclovir treatment in the eye upregulated several cytokines related to NKT and T-cell responses (IL-1 $\alpha$ , IL-2, IL-18, TNF- $\alpha$ ) in the anterior segment and T-cell responses in the lymph nodes indicates that a stronger immune surveillance can be established with early antiviral treatment. These findings also imply that CMV infection may suppress the immune defense through downregulation of cytokines. Nonetheless, the mechanism of this immune escape and how CMV may interplay with infected anterior segment tissues necessitates further investigation.

## CONCLUSIONS

We demonstrated that the inoculation method could represent a robust model for characterizing primary CMV eye infection in immunocompetent hosts (Fig. 8). Our results showed that the elevation of IOP and gradual clearance of virus DNA in the anterior segment coincided with an inhabiting cascade of ocular immune cells resulting from the sequential development of innate and adaptive immunity against CMV infection. Antiviral drug ganciclovir treatment augmented release of cytokines that boost T-cell response and facilitate recruitment of NKT and T cells in drainage lymph nodes to contain the virus. Glucocorticoid treatment, alone or combined with ganciclovir treatment, decreased elevation of IOP but also impeded DNA clearance. These results suggest that the use of GC in current practice may hinder the viral clearance and that ganciclovir treatment can facilitate cytokine expression to combat the virus.

## Acknowledgments

The authors thank the staff of the Second Core Lab and the Third Core Lab, Department of Medical Research, National Taiwan University Hospital for technical support.

Supported by grants from the Ministry of Science and Technology (110-2634-F-002-044, 105-2314-B-002-033, 106-2314-B1-002-130-MY3, 106-2314-B-002-124-MY3) and the National Taiwan University Hospital (106-N3680, 107-M4045, 108-M4326, 108-S4420, 109-M4696, 109-S4787, 110-M5047).

Disclosure: C.-C. Su, None; C.-M. Gao, None; F.-T. Peng, None; T.-S. Jou, I.-J. Wang, None

## References

- Koizumi N, Suzuki T, Uno T, et al. Cytomegalovirus as an etiologic factor in corneal endotheliitis. *Ophthalmology*. 2008;115:292-297.
- Chee SP, Bacsal K, Jap A, Se-Thoe SY, Cheng CL, Tan BH. Clinical features of cytomegalovirus anterior uveitis in immunocompetent patients. *Am J Ophthalmol*. 2008;145:834-840.
- Shiraishi A, Hara Y, Takahashi M, et al. Demonstration of "owl's eye" morphology by confocal microscopy in a patient with presumed cytomegalovirus corneal endotheliitis. *Am J Ophthalmol*. 2007;143:715-717.
- Kawaguchi T, Sugita S, Shimizu N, Mochizuki M. Kinetics of aqueous flare, intraocular pressure and virus-DNA copies in a patient with cytomegalovirus iridocyclitis without retinitis. *Int Ophthalmol* 2007;27:383-386.
- Su CC, Hu FR, Wang TH, et al. Clinical outcomes in cytomegalovirus-positive Posner-Schlossman syndrome patients treated with topical ganciclovir therapy. *Am J Ophthalmol*. 2014;158:1024-1031.
- Choi JA, Kim JE, Noh SJ, et al. Enhanced cytomegalovirus infection in human trabecular meshwork cells and its implication in glaucoma pathogenesis. *Sci Rep*. 2017;7:43349.
- Voigt V, Andoniou CE, Schuster IS, et al. Cytomegalovirus establishes a latent reservoir and triggers long-lasting inflammation in the eye. *PLoS Pathog*. 2018;14(5):e1007040.
- Bale JF, Jr., O'Neil ME, Folberg R. Murine cytomegalovirus ocular infection in immunocompetent and cyclophosphamide-treated mice. Potentiation of ocular infection by cyclophosphamide. *Invest Ophthalmol Vis Sci*. 1991;32:1749-1756.
- Sandford GR, Ho K, Burns WH. Characterization of the major locus of immediate-early genes of rat cytomegalovirus. *J Virol*. 1993;67:4093-4103.
- Li J, Lin L, Du L, et al. Radioprotective effect of a pan-caspase inhibitor in a novel model of radiation injury to the nucleus of the abducens nerve. *Mol Med Rep*. 2014;10(3):1433-1437.
- Chee SP, Jap A. Presumed Fuchs heterochromic iridocyclitis and Posner-Schlossman syndrome: comparison of cytomegalovirus-positive and negative eyes. *Am J Ophthalmol*. 2008;146:883-889.
- Koizumi N, Yamasaki K, Kawasaki S, et al. Cytomegalovirus in aqueous humor from an eye with corneal endotheliitis. *Am J Ophthalmol*. 2006;141:564-565.
- Takeuchi T, Fujii A, Okumiya T, et al. The study of cytopathological aspects induced by human cytomegalovirus infection. *Diagn Cytopathol*. 2004;31:289-293.
- Tuailon N, Shen DF, Berger RB, Lu B, Rollins BJ, Chan CC. MCP-1 expression in endotoxin-induced uveitis. *Invest Ophthalmol Vis Sci*. 2002;43:1493-1498.
- Liu B, Mori I, Hossain MJ, Dong L, Takeda K, Kimura Y. Interleukin-18 improves the early defense system against influenza virus infection by augmenting natural killer cell-mediated cytotoxicity. *J Gen Virol*. 2004;85:423-428.
- Kobayashi A, Yokogawa H, Higashide T, Nitta K, Sugiyama K. Clinical significance of owl eye morphologic features by in vivo laser confocal microscopy in patients with

- cytomegalovirus corneal endotheliitis. *Am J Ophthalmol.* 2012;153:445–453.
17. Camelo S, Kezic J, Shanley A, Rigby P, McMenamin PG. Antigen from the anterior chamber of the eye travels in a soluble form to secondary lymphoid organs via lymphatic and vascular routes. *Invest Ophthalmol Vis Sci.* 2006;47:1039–1046.
  18. Hoffmann F, Zhang EP, Mueller A, et al. Contribution of lymphatic drainage system in corneal allograft rejection in mice. *Graefes Arch Clin Exp Ophthalmol.* 2001;239:850–858.
  19. Townsend WM, Kaufman HE. Pathogenesis of glaucoma and endothelial changes in herpetic kerato-uveitis in rabbits. *Am J Ophthalmol.* 1971;71:904–910.
  20. Deshmane SL, Kremlev S, Amini S, Sawaya BE. Monocyte chemoattractant protein-1 (MCP-1): an overview. *J Interferon Cytokine Res.* 2009;29:313–326.
  21. Hokeness-Antonelli KL, Crane MJ, Dragoi AM, Chu WM, Salazar-Mather TP. IFN-alpha beta-mediated inflammatory responses and antiviral defense in liver is TLR9-independent but MyD88-dependent during murine cytomegalovirus infection. *J Immunol.* 2007;179:6176–6183.
  22. Crane MJ, Hokeness-Antonelli KL, Salazar-Mather TP. Regulation of inflammatory monocyte/macrophage recruitment from the bone marrow during murine cytomegalovirus infection: role for type I interferons in localized induction of CCR2 ligands. *J Immunol.* 2009;183:2810–2817.
  23. Loh J, Chu DT, O'Guin AK, Yokoyama WM, HWt Virgin. Natural killer cells utilize both perforin and gamma interferon to regulate murine cytomegalovirus infection in the spleen and liver. *J Virol.* 2005;79:661–667.
  24. Vliegen I, Duijvestijn A, Stassen F, Bruggeman C. Murine cytomegalovirus infection directs macrophage differentiation into a pro-inflammatory immune phenotype: implications for atherogenesis. *Microbes Infect.* 2004;6:1056–1062.
  25. Hodge DL, Subleski JJ, Reynolds DA, et al. The proinflammatory cytokine interleukin-18 alters multiple signaling pathways to inhibit natural killer cell death. *J Interferon Cytokine Res.* 2006;26:706–718.
  26. Rook AH, Masur H, Lane HC, et al. Interleukin-2 enhances the depressed natural killer and cytomegalovirus-specific cytotoxic activities of lymphocytes from patients with the acquired immune deficiency syndrome. *J Clin Invest.* 1983;72:398–403.
  27. Wesley JD, Tessmer MS, Chaukos D, Brossay L. NK cell-like behavior of Valpha14i NK T cells during MCMV infection. *PLoS Pathog.* 2008;4(7):e1000106.
  28. Eberl G, MacDonald HR. Rapid death and regeneration of NKT cells in anti-CD3epsilon- or IL-12-treated mice: a major role for bone marrow in NKT cell homeostasis. *Immunity.* 1998;9:345–353.
  29. Leite-De-Moraes MC, Hameg A, Arnould A, et al. A distinct IL-18-induced pathway to fully activate NK T lymphocytes independently from TCR engagement. *J Immunol.* 1999;163:5871–5876.
  30. Egan RM, Yorkey C, Black R, Loh WK, Stevens JL, Woodward JG. Peptide-specific T cell clonal expansion in vivo following immunization in the eye, an immune-privileged site. *J Immunol.* 1996;157:2262–2271.
  31. McKenna KC, Xu Y, Kapp JA. Injection of soluble antigen into the anterior chamber of the eye induces expansion and functional unresponsiveness of antigen-specific CD8+ T cells. *J Immunol.* 2002;169:5630–5637.
  32. Niederkorn JY, Lynch MG. Reconsidering the immunologic privilege and lymphatic drainage of the anterior chamber of the eye. *Transplant Proc.* 1989;21:259–260.
  33. Beato M, Herrlich P, Schutz G. Steroid hormone receptors: many actors in search of a plot. *Cell.* 1995;83:851–857.
  34. Pavan-Langston D, Geary PA. Steroid inhibition of leukocyte defense system in mycoplasmal uveitis. *Arch Ophthalmol.* 1971;86:575–582.
  35. Su CC, Wang IJ, Chen WL, Lin CP, His B, Hu FR. Topical ganciclovir treatment in patients with cytomegalovirus endotheliitis receiving penetrating keratoplasty. *Clin Exp Ophthalmol.* 2013;41:339–347.
  36. Matthews T, Boehme R. Antiviral activity and mechanism of action of ganciclovir. *Rev Infect Dis.* 1988;10(Suppl 3):S490–S494.